Geophysical Journal International

Geophys. J. Int. (2016) **206,** 731–741
Advance Access publication 2016 April 26
GJI Geodynamics and tectonics

doi: 10.1093/gji/ggw166

The Manihiki Plateau—a key to missing hotspot tracks?

R. Pietsch and G. Uenzelmann-Neben

Alfred Wegener Institute Helmholtz Centre for Polar and Marine Research, Postfach 120161*, D-*27515 *Bremerhaven, Germany.*
E-mail: ricarda.pietsch@awi.de

Accepted 2016 April 22. Received 2016 April 18; in original form 2015 November 26

SUMMARY

A Neogene magmatic reactivation of the Manihiki Plateau, a large igneous province (LIP) in the central Pacific, is studied using seismic reflection data. Igneous diapirs have been identified exclusively within a narrow WNW–ESE striking corridor in the southern High Plateau (HP), which is parallel to the Neogene Pacific Plate motion and overlaps with an extrapolation of the Society Islands Hotspot (SIH) path. The igneous diapirs are characterized by a narrow width (>5 km), penetration of the Neogene sediments, and they become progressively younger towards the East (23–10 Ma). The magmatic source appears to be of small lateral extent, which leads to the conclusion that the diapirs represent Neogene hotspot volcanism within a LIP, and thus may be an older, previously unknown extension of the SIH track (>4.5 Ma). Comparing hotspot volcanism within oceanic and continental lithosphere, we further conclude that hotspot volcanism within LIP crust has similarities to tectonically faulted continental crust.

Key words: Oceanic hotspots and intraplate volcanism; Submarine tectonics and volcanism; Hotspots; Large igneous provinces; Pacific Ocean.

1 INTRODUCTION

Intraplate, age progressive, volcanic hotspot chains have been the focus of research due to their importance for understanding mantle dynamics, including the source and behaviour of time dependent intraplate volcanism. They have been used as an important tool, for example as a reference frame in absolute plate motion models (e.g. Wessel *et al.* 2006; Wessel & Kroenke 2008), which are used in plate reconstruction models (e.g. Chandler *et al.* 2012; Seton *et al.* 2012).

Different explanation models exist for intraplate hotspot chains, whose cause is still debated. On the one hand, hotspots are believed to display surface expressions of hot, rising mantle plumes that emplace a linear chain of volcanoes on a plate moving overhead and which originate from a boundary layer within the Earth's mantle (Morgan 1972). An alternative view is that hotspot volcanism represents shear-stress driven upwelling within the lithosphere (e.g. Hieronymus & Bercovici 2000; Ballmer *et al.* 2013) due to hotspot-ridge interaction (Kopp *et al.* 2003; O'Connor *et al.* 2015) and due to changes in slab-pull forces induced by plate-re-organization (Wessel & Kroenke 2007), intraplate volcanism as a by-product of plate tectonics itself (e.g. Anderson 2000; Foulger & Natland 2003), or hotspot volcanism as precursor for a break-apart of the Pacific Plate (Clouard & Gerbault 2008). To gain a better understanding of hotspot chains and their origin, it is important to investigate areas where geological evidence is subdued and hotspot paths have been extrapolated so far.

The Pacific Ocean provides a suitable terrain to study hotspot volcanism, that is along the Emperor-Hawaii Hotspot track in the North, the Samoa, Society Islands, Tahiti, Pitcairn, Marshall-Gilbert, Austral-Cook and McDonald Hotspot tracks in the central Pacific and the Louisville Hotspot track in the south (Fig. 1a). Various tomographic, geochemical, petrological and geodynamic studies have been carried out (e.g. Binard *et al.* 1993; Gaboret *et al.* 2003; Barruol *et al.* 2009; Suetsugu *et al.* 2009; Tanaka *et al.* 2009a,b; Adam *et al.* 2010; Suetsugu & Hanyu 2013); however, a uniform, straight forward and complete model has remained elusive. Still under discussions are explanations for track bends of different orientations and ages seen for different hotspot tracks, such as the Hawaiian Hotspot bend (47 Ma; Sharp & Clague 2006) vs the Marshall-Gilbert Hotspot bend (67 Ma) and Tokelau seamount bend (57 Ma; Koppers & Staudigel 2005; Koppers *et al.* 2007). Absent signs of long, continuous hotspot tracks in the central Pacific are further challenging in order to connect the western and eastern Pacific hotspot tracks, for example the Society Islands only comprise a short island and archipelago track with an age of 4.5–0 Ma (Duncan & McDougall 1976; Clouard & Bonneville 2001; Koppers *et al.* 2003).

In this study, we have investigated Neogene magmatism seen across the Manihiki Plateau (MP), a large igneous province (LIP) in the central Pacific (Fig. 1b). We have used seismic reflection data gathered during cruise So224 (Uenzelmann-Neben 2012; Pietsch & Uenzelmann-Neben 2015) and cruise Kiwi12 (Ai *et al.* 2008; Fig. 1d) to answer the following questions: (1) can Neogene hotspot magmatism be identified for the MP, (2) has the Neogene magmatism induced tectonic activity and (3) in what way is the appearance of magmatism within the LIP different to that observed for the surrounding oceanic plate?

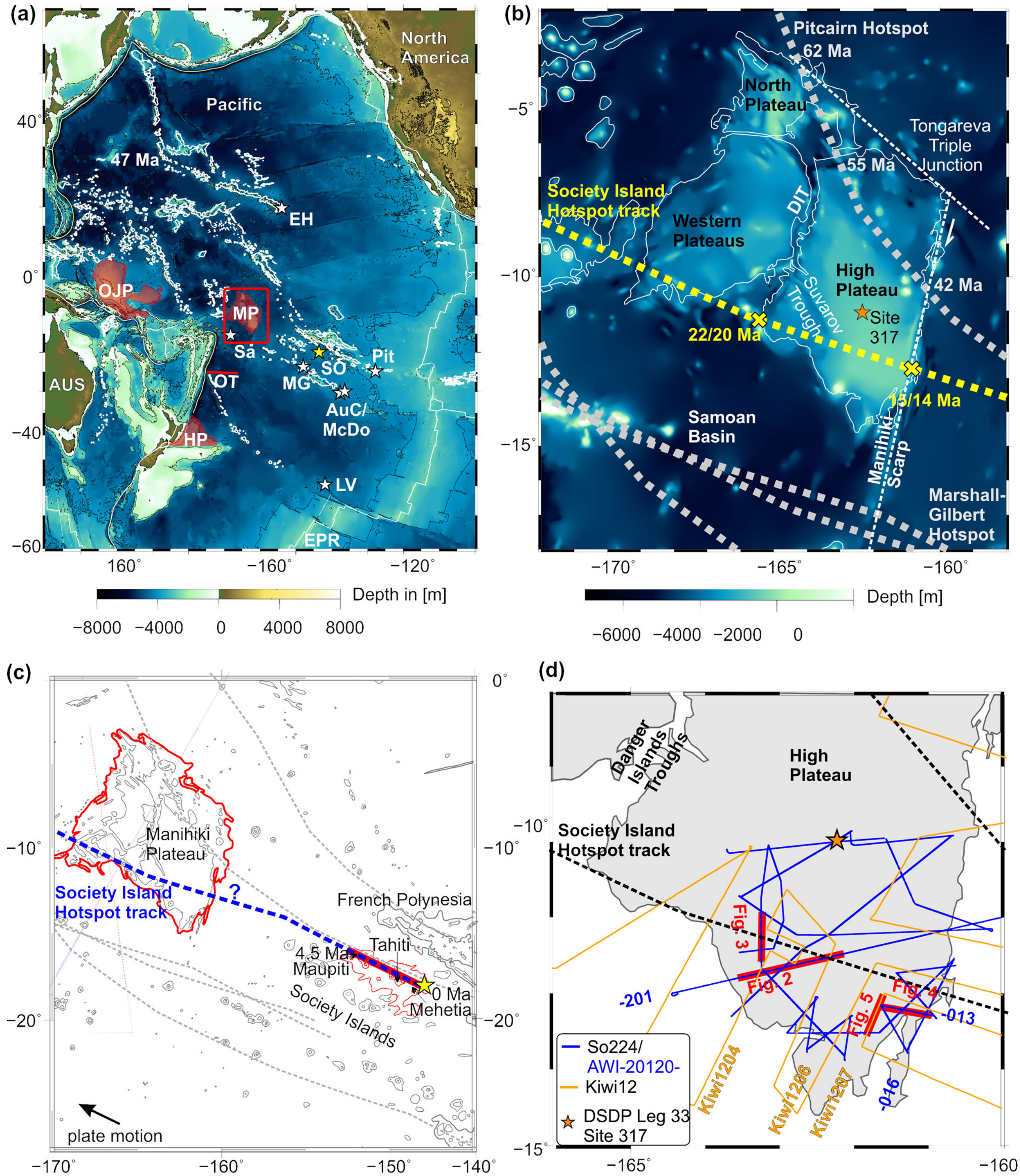

Figure 1. Geological context of Pacific Large Igneous Provinces. (a) Large Igneous Provinces: OJP, Ontong Java Plateau; MP, Manihiki Plateau and HP, Hikurangi Plateau (red shaded) and hotspot tracks in the Pacific Ocean on top of General Bathymetric Chart of the Oceans (GEBCO; Weatherall *et al.* 2015) bathymetry with most recent hotspot centres (white stars); EH, Emperor-Hawaiian Hotspot; SO, Society Islands Hotspots (yellow star); Pit, Pitcairn Hotspot; Sa, Samoan Hotspot; MG, Marshall-Gilbert Hotspot; AuC/McDo are Austral-Cook and McDonald hotspots, respectively, LV, Louisville hotspot. Red box marks area of investigation. OT, Osbourn Trough, a palaeo-spreading centre (Billen & Stock 2000), EPR, East Pacific Rise. (b) Enlargement of the area of investigation, the Manihiki Plateau with its subprovinces the North Plateau, Western Plateaus and High Plateau, separated by the Danger Islands Troughs (DIT). Interpolated hotspot tracks of WK08-D (Wessel & Kroenke 2008) are shown in dashed yellow (Society Islands Hotspot track) and dashed grey lines. Pitcairn and Society Islands Hotspots crossed the High Plateau between 57–42 Ma and 22/20-15/14 Ma, respectively. Orange star marks location of DSDP Leg 33 Site 317 (Shipboard Scientific Party 1976). (c) Enlargement of central Pacific area; Manihiki Plateau and the Society Islands within French Polynesia are highlighted in red. Blue dashed line underlined in red is previously dated seamounts of the Society Islands Hotspot (yellow star) with postulated continuation, same as in (b). (d) Location of single channel reflection data of cruise Kiwi12 (orange lines) and multichannel seismic reflection data of cruise So224 (blue lines) across the High Plateau. Orange star is same as in Fig. 1(b). Red highlighted parts of profiles display locations of Figs 2–5.

2 GEOLOGICAL BACKGROUND

2.1 The Manihiki Plateau

The MP is a LIP located in the central Pacific and comprises three subplateaus: the North Plateau, the Western Plateaus and the High Plateau (Figs 1a and b). It has been proposed to be the centrepiece of Ontong Java Nui, a Super-LIP, because it was connected to the Ontong Java Plateau (OJP) in the west, the Hikurangi Plateau in the South and two subducted fragments in the East (Taylor 2006; Chandler *et al.* 2012; Hochmuth *et al.* 2015; Pietsch & Uenzelmann-Neben 2015; Hochmuth *et al.*, in preparation). It was emplaced during three volcanic phases in the early Cretaceous: the initial formation phase (>125 Ma), followed by the expansion phase (∼125–116 Ma) and secondary volcanism (∼110–65 Ma; Pietsch & Uenzelmann-Neben 2015). During the expansion phase, previously referred to as main formation phase, massive eruptions of tholeiitic basalts occurred (Lanphere & Dalrymple 1976; Shipboard Scientific Party 1976; Mahoney *et al.* 1993; Larson & Erba 1999; Hoernle *et al.* 2010; Timm *et al.* 2011), resulting in anomalously thick oceanic crust (Hussong *et al.* 1979) that comprises a thickness up to 20 km on the High Plateau (Hochmuth *et al.*, in preparation). Secondary volcanism (∼100–65 Ma) consisted of alkaline volcaniclastics (Ingle *et al.* 2007; Hoernle *et al.* 2010; Timm *et al.* 2011), which broadened and flattened the topographic appearance of the High Plateau and preferentially occurred at the margins of the High Plateau (Pietsch & Uenzelmann-Neben 2015).

At the end of the expansion phase, the MP crust broke up into separate tectonic sectors, leading to the development of the three MP subprovinces. In the west, the Danger Islands Troughs separate the Western Plateaus from the High Plateau (Fig. 1b). They were either formed in an sinistral strike-slip tectonic environment (Nakanishi *et al.* 2015) or comprise a series of pull-apart structures, which were formed as a failed rift system when the Ontong-Java Plateau broke-off the Western Plateaus around 118 Ma (Taylor 2006). In the north, the Pacific-Farallon-Phoenix triple junction jumped to the newly formed MP and developed the Tongareva triple junction at 119 Ma with average spreading rates of 18–20 cm yr^{-1} until 84 Ma (Larson *et al.* 2002). The Manihiki Scarp, a ridge and trough system at the eastern margin of the High Plateau, developed from north to south by strike-slip (transform) motion. It displays the break-up of two fragments, which were connected to the MP during the expansion phase (>120 Ma; Pietsch & Uenzelmann-Neben 2015) and rifted away on the Farallon and Phoenix Plates (Larson *et al.* 2002; Hochmuth *et al.* 2015). Leaky rifting with volcanic overprinting (secondary volcanism) continued at the southern Manihiki Scarp until 65 Ma (Pietsch & Uenzelmann-Neben 2015).

The morphology of the southern and southwestern part of the High Plateau is characterized by stretched and rifted crustal structures, which were initiated by the break-up of the Manihiki-Hikurangi Plateau (Ai *et al.* 2008; Pietsch & Uenzelmann-Neben 2015) at the Osbourn Trough ∼118 Ma and ceased when the Hikurangi Plateau collided with a southward-dipping subduction system along the Gondwana Margin at ∼100 Ma (eastern New Zealand; Worthington *et al.* 2006; Davy *et al.* 2008; Davy 2014). Fault systems occurred, showing deformation of the sequences associated with the LIP formation, particularly in the southern High Plateau and the western and eastern margins, whereas the northern High Plateau remained undisturbed (Pietsch & Uenzelmann-Neben 2015). They show tectonic faulting of the basement after the initial formation period (∼65–45 Ma), probably caused by Pacific Plate reorganization (Pietsch & Uenzelmann-Neben 2016). Since the middle Eocene, tectonism and magmatism of the MP has become quiet until a Neogene magmatic activity occurred, which is discussed in here.

2.2 Society Islands Hotspot chains in the central Pacific

Fourteen hotspots are generally considered to have been existent within the Pacific Ocean and are grouped into (i) classical hotspots, long-lasting hotspots that are believed to be generated by deep rising mantle plumes (e.g. Louisville Hotspot and Hawaiian Hotspot) and (ii) short lived hotspots (<35 Ma, e.g. Samoa, Society Islands and Pitcairn; Clouard & Bonneville 2001). We focus on the Society Islands Hotspot (SIH), which the MP likely passed over during the Cenozoic (Figs 1b and c).

The Society Islands, located in French Polynesia, are aligned along a volcanic chain parallel to the Pacific plate motion (Gripp & Gordon 1990; Gripp & Gordon 2002) and perpendicular to the East Pacific Rise (Duncan & McDougall 1976). The NW to SE striking archipelago comprises more than 14 islands along a 400-km-long volcanic track (Duncan & McDougall 1976; Binard *et al.* 1991; Neall & Trewick 2008). An age progression occurs from southeast to northwest, from the recently active Mehetia Island (Binard *et al.* 1991, 1993; Uto *et al.* 2007), where the SIH is assumed to be located, over Tahiti Island (0.48–1.23 Ma) to the oldest and extinct Maupiti Island (4.5 Ma; Duncan & McDougall 1976). No bathymetrical evidence has so far been reported for a western extent of the SIH (Clouard & Bonneville 2001).

3 DATA ACQUISITION AND SEISMIC STRATIGRAPHY

Single channel seismic reflection data (SCS) of cruise Kiwi12 (Ai *et al.* 2008) and high resolution multichannel seismic reflection data (MCS) gathered during cruise So224 (Uenzelmann-Neben 2012) covering the High Plateau (Figs 1b and c) and the surrounding basins serve as basis for this study. Kiwi12 SCS data were gathered using two 210 cubic inch air guns, a firing interval of 10 s, a recording length of 7 s, and an average trace interval spacing of 45 m (Ai *et al.* 2008). So224 MCS data were collected using a cluster of four GI-guns (volume 45 in^3 + 105 in^3), which were fired at a depth of 2 m with a shot interval of 10 s (∼25 m). For profile AWI-20120201, a cluster of eight G-Guns (total volume 4160 in^3) at a depth of 10 m was used with a shot interval of 60 s. Data were recorded with a 3 km long, 240-channel streamer (Sercel SEAL™) at a sampling rate of 1 ms (2 ms for line AWI-20120201). A frequency range up to 250 Hz allowed for a maximum vertical resolution of about ∼3 m at the ocean bottom (Uenzelmann-Neben 2012; Pietsch & Uenzelmann-Neben 2015). Processing steps for the MCS data included Common Depth Point sorting (CDP), analyses of velocity–time profiles every 50th CDP, Normal-Move-Out correction, stacking and time migration.

We correlated the MCS data to data of Deep Sea Drilling Project (DSDP) Leg 33 Site 317 (Shipboard Scientific Party 1976) by calculating a synthetic seismogram (Pietsch & Uenzelmann-Neben 2015). The correlation is summarized in Table 1. Seven reflections R1–R7 have been identified (Table 1). The sedimentary column has been divided into four units. Sediments of Units 1 and 2 include Quaternary calcareous ooze to Late Eocene chalk, bounded by unconformities R5/U1 and R6/U2, respectively. Units 3 and 4 encompass Cretaceous basaltic lavas and volcaniclastic deposits. The crossing of CATO3 and So224 (Pietsch & Uenzelmann-Neben

Table 1. Defined seismostratigraphic model based on SCS reflection data of cruise Kiwi12 (Ai *et al.* 2008) and MCS reflection data of cruise So224 (Uenzelmann-Neben 2012) and lithology of borehole DSDP Leg 33 Site 317 (Shipboard Scientific Party 1976). For details on correlation see (Pietsch & Uenzelmann-Neben 2015).

Seismic units	DSDP Leg 33 Site 317 Lithology	Depth (mbsf)[a]	Age (Ma)	So224 Refl. name	Depth TWT (s)	Int. vel. (km s^{-1})	Interpretation this paper
Unit 1	Calc. ooze	0	1.8	**R1**	3.46		Seafloor;
	Calc. ooze	58	5.3	**R2**	3.53	1.6–1.7	Pelagic sedimentation
	Ooze to Chalk	140	10	**R3**	3.63	1.7–1.9	
	Chalk	197	23	**R4**	3.68	2.0	
Unit 2	Ooze to chalk limestone chert	**358**	45	**R5**	3.88	1.7–2.1	358 m late Eocene-mid Eocene unconformity corresponds to accumulation rate change; Pelagic sedimentation
	Drilling gap	377?	∼55?	**R5a**	3.94		Core sections above and below show Eocene to Cretaceous chalks
Unit 3	Sandstone-siltstone, claystone, limestone, volcaniclastic	**576**	65	**R6**	4.05	2.5–3.0	Maestrichtian-Campanian boundary; Secondary volcanic phase
	Cretaceous limestone with minor chalk, claystone and chert	592 ∼602–645?					
	Volcaniclastics	**680**	∼100[b]	**R6a**	4.22	2.0–2.5	Transition from tholeiitic to alkalic volcaniclastics
Unit 4a	Basalt	910	116–120	**R7**	4.33	3.5–4.0	Top of basalt; Volcanic expansion phase
Unit 4b			>125?	**IB1**	4.95	5–5.7	Intrabasement reflection sequence, initial formation phase

[a]mbsf: metres below sea floor.
[b]Age refers to change from tholeiitic basalts to alkalic lavas (Ingle *et al.* 2007).

2015) profiles with the DSDP Leg 33 Site 317 allowed a lateral expansion of the seismic stratigraphy, which was used to correlate to the Kiwi12 at the crossing lines.

4 RESULTS

4.1 Identification of Neogene magmatism

The MP was formed by massive volcanism. Those volcanic structures associated with the Cretaceous LIP formation - the initial formation phase (>125 Ma), the expansion phase (∼125–116 Ma), and secondary volcanism (110–65 Ma), which are correlated to Units 4b (>IB1), Unit 4a (IB1–R7) and Unit 3 (R7–R6), respectively, (Table 1) have been discussed by Pietsch & Uenzelmann-Neben (2015). The seismic sequences associated with this period are marked as a reference in purple in Figs 2, 3, 5 and 6. Here, we focus on small magmatic structures seen as diapirs within the sedimentary column, which deformed the Cenozoic sedimentary sequences and hence occurred after the initial emplacement period.

4.1.1 Characterization of Cenozoic diapirs

Diapirs, also referred to as piercement structures, are common features within the deep sea (Lancelot & Embley 1977). They are generally associated with (1) synclinal depressions between the piercements, (2) doming of the surficial sediments, (3) faulting of the surficial sediments and (4) plugs of non-reflective zones in the surficial sediments (Lancelot & Embley 1977). We have identified the igneous diapirs using these characteristics seen in seismic reflection data (Figs 2–5), especially amplitude attenuation within the structure compared to the surrounding strata and deformation of sedimentary sequences. We further classified the features into extrusion and intrusion centres.

Lateral and vertical reflection amplitude changes occur within a diapir compared to the adjacent area due to an intrusion of material from below that is characterized by higher *P*-wave velocities (e.g. CDPs 7600–7650 and 7000–7050 in Fig. 2, CDPs 1550–1650 in Fig. 3), which is indicated by the pull-up effect within the structure (Jackson 2012). In particular, a decrease or loss of amplitude with lateral extent between 1.3 and 5 km occurs in the MCS data (e.g. CDP 7600–7650 in Fig. 2). The vertical extent of plugs with amplitude loss or decrease comprise Units 2 (R5–R6), 3 (R6–R7) and 4 (>R7) and varies regionally.

The edges of at least Units 3 and 4, partly of Unit 2 at the diapir are deflected (e.g. CDP 1500–1650 in Fig. 3). These deformations indicate an existence of the sedimentary sequences before the formation of the diapir and hence indicate a oldest formation age. The youngest deformed horizon (e.g. reflection R3 at CDPs 1250–1350 in Fig. 3) is an indication for the minimum time of formation, as it specifies the sedimentary

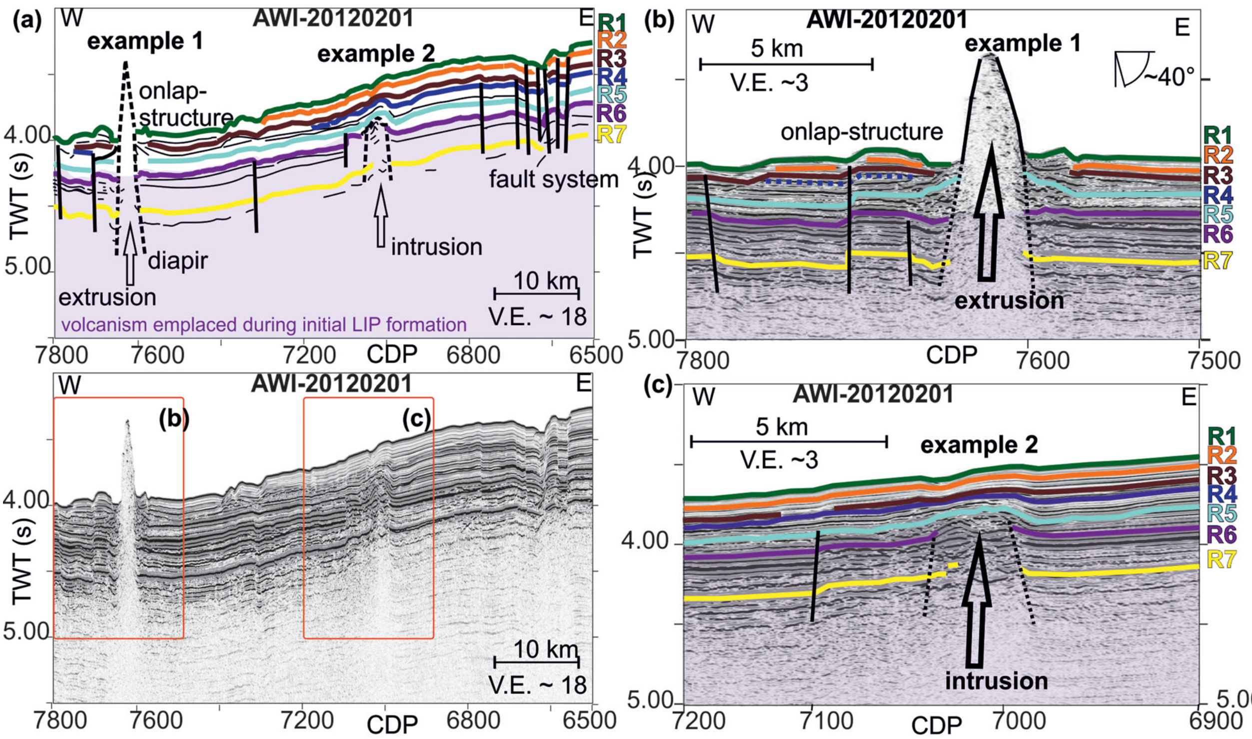

Figure 2. Part of seismic profile AWI-20120201 in the southwestern part of the High Plateau in (a) an uninterpreted and interpreted version, (b) enlargement of extrusion centre (example 1) and (c) intrusion centre (example 2). Coloured reflections are defined reflections R1–R7 of Table 1.

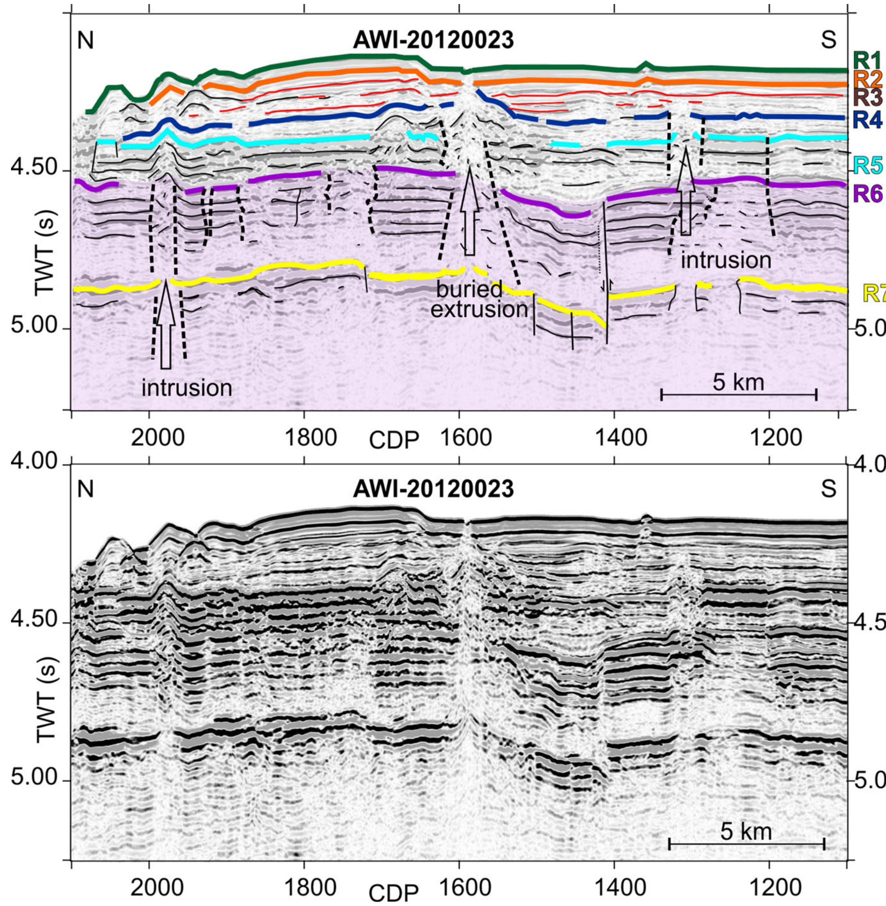

Figure 3. Northwest–southeast striking seismic profile AWI-20120023 uninterpreted (bottom) and interpreted (top) version with identified reflections R1–R7.

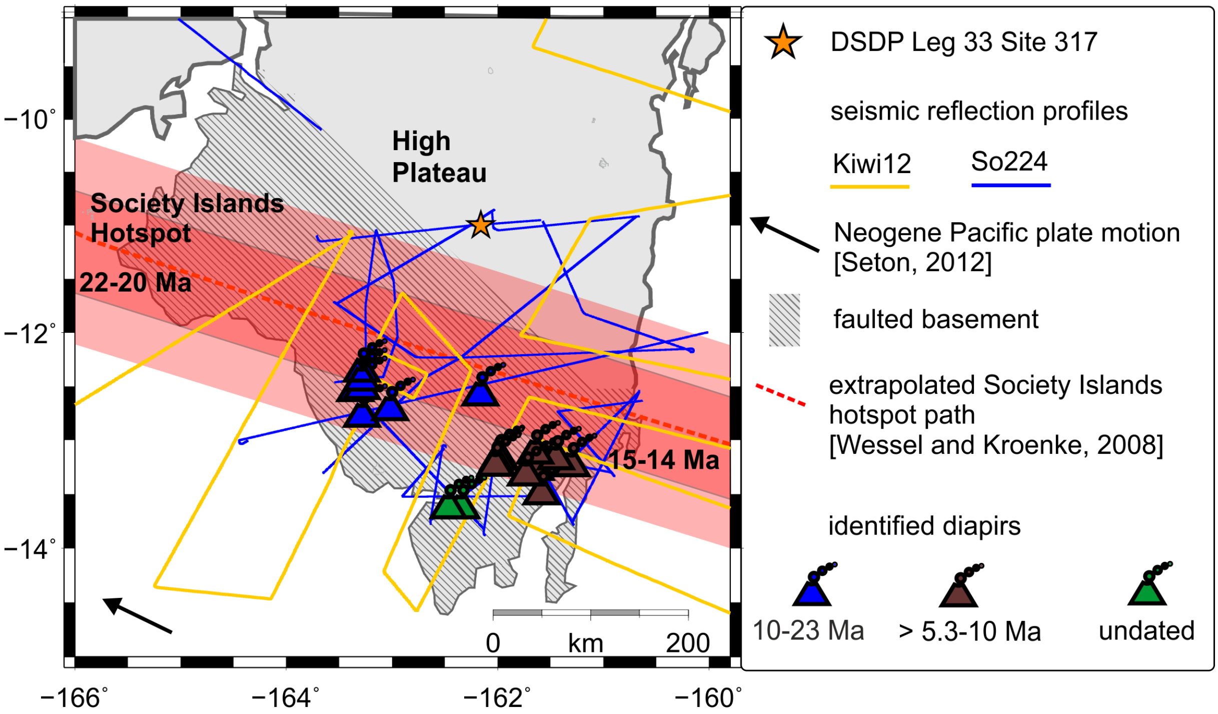

Figure 4. Seismic profiles of cruises Kiwi12 (orange) and So224 (blue) across the High Plateau subplateau of the Manihiki Plateau, with tectonically faulted crust (hatched area). Spatial distribution of identified intrusion centres with an estimated formation age of 10–23 Ma (blue) and >5.3–10 Ma (brown) and undated volcanoes (green) are displayed. Extrapolated hotspot tracks of absolute plate motion model WK08-D (Wessel & Kroenke 2008) with 50 and 100 km uncertainty are shown in red.

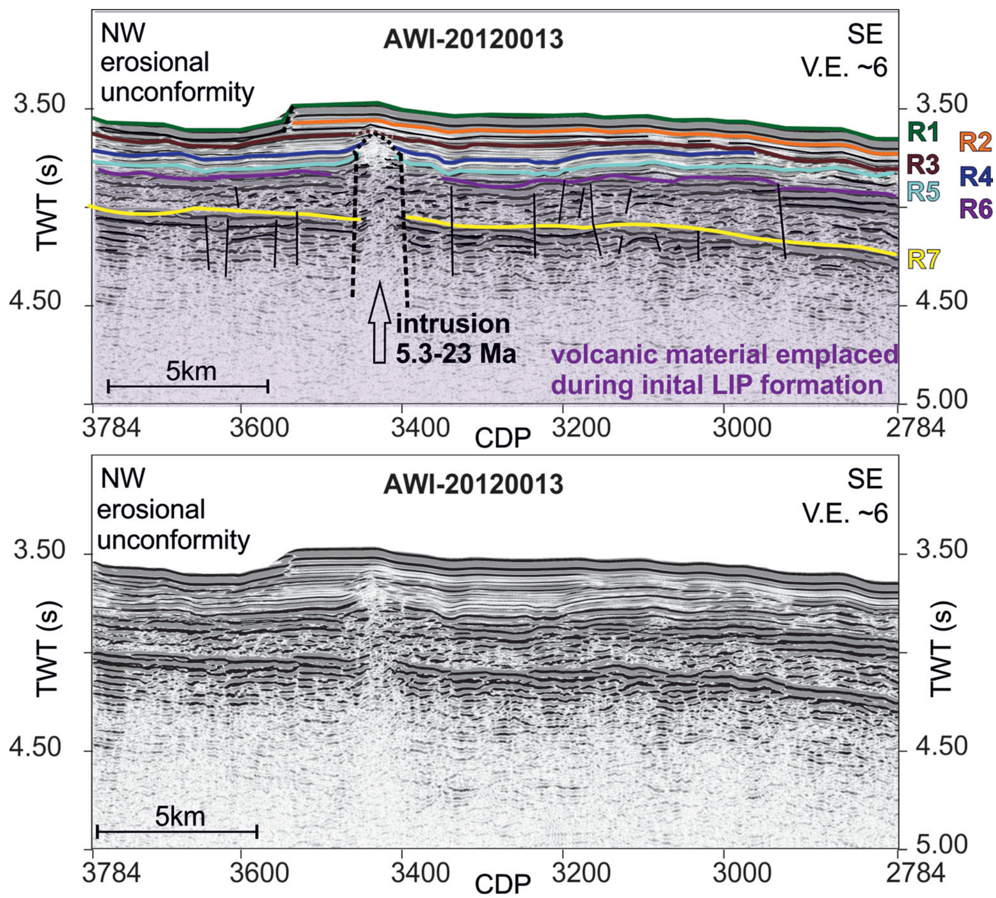

Figure 5. Seismic profiles AWI-20120013 in the southeastern part of the High Plateau with highlighted reflections R1–R7.

sequences, which have already been accumulated before the diapir was formed.

The magmatic diapirs either represent extrusive or intrusive features. Extrusive diapirs (e.g. CDP 7600–7650 in Fig. 2) have penetrated the entire sedimentary column up to the seafloor and exhibit bathymetric highs with steep flanks up to ~40° (Fig. 2b). Onlap-structures can be observed (reflection R3 in Fig. 2), which indicate a development of these sequences after the diapir was formed and hence provide a youngest formation age estimation. Eocene to Miocene intrusion centres are identified if they penetrate at least the volcanic Units 3 and 4 and show doming of surficial sediments of sedimentary Units 1–2 (e.g. CDP 6980–7100 in Fig. 2c). The uppermost penetrated and disturbed reflection sequence provides the oldest formation age. The sedimentary structure of the above lying, domed sediments hint towards a pelagic sedimentation after the diapir was formed.

4.1.2 *Regional differences of the identified diapirs*

A total number of 19 magmatic diapirs has been identified using the above listed characteristics and has been summarized in Table 2. They are distributed in a ~100 km wide corridor crossing the southern High Plateau from WNW to ESE (Fig. 4) and can be split into a southwestern and southeastern cluster based on their location and age. The southwestern cluster encompasses an areal extent of ~100 km NS by ~50 km EW (blue volcanoes in Fig. 4) and the southeastern cluster an areal extent of ~100 km NS by ~150 km EW (brown volcanoes in Fig. 4).

In the southwestern part of the High Plateau, eight distinct diapirs are located along profiles AWI-20120201/-028/-023 and Kiwi1204 (Fig 1c for overview of profiles, 2, 3 and 4) and have lateral extents between 1.3 and 4 km (Table 2). For these extrusion centres (profile AWI-20120201 and AWI-20120023) the earliest onlap structures occur between reflections R3 (brown) and R4 (dark-blue; Fig. 2 and red reflections Fig. 3). The intrusion centres show disturbances of reflection R5 and locally reach reflection R4, whereas the above lying sequences show no disturbances (e.g. profile AWI-20120201, Fig. 2). This finding points towards a formation simultaneously to the accumulation of reflections R4–R3.

In the southeast of the High Plateau, nine diapirs have been identified on profiles AWI-20120013/-016 and Kiwi1206 and Kiwi1207 (Figs 1d, 4, 5 and 6). The extrusions and intrusions have a lateral extent between 1.8 and 5 km (Table 2). They show amplitude disturbances within Units 2–4 (Reflection R5→R7 in Figs 5 and 6), with a deflection of the edges that indicate a pre-existence of these units. Additionally, smaller disturbances occur within reflections R3 and R4 and cease between reflections R2 and R3 (e.g. profile Kiwi1207 in Fig. 6), which represent the youngest formation of the diapir.

5 DISCUSSION

5.1 Are observed igneous diapirs an expression of hotspot volcanism?

To investigate whether the igneous diapirs represent hotspot volcanism or a reactivation of a Cretaceous magma chamber that remained beneath the central High Plateau, we will discuss if the diapirs show hotspot characteristics, which are a (linear) age progression, and a distribution in a corridor parallel to the plate motion. We are not able to investigate and discuss the chemical hotspot characteristics, as no petrological data are available.

5.1.1 *Age determination*

All diapirs within the southwestern cluster (Figs 2, 3 and 6) show strong disturbances of Units 2–4 (R5–R7) and are therefore of younger age than 45 Ma (R5). The youngest formation ages can be estimated from the termination of deformed sequences or from the lower boundaries of onlap-structures adjacent to the extrusion centres, which developed after the diapir was formed. The onlap-structures can be observed within Unit 1, which includes sequences bounded by reflections R5–R3 (profile AWI-20120201, Fig. 2b) and reflections R4–R2 (red reflections in Fig. 3). Therefore, approximate formation ages range between 23 and 10 Ma.

Diapirs identified within the southeastern cluster show disturbances within Units 2–4, and deformations of reflections R4 and partly R3, which terminate between reflections R3–R2. Therefore, they formed between ~10 and >5.3 Ma and are thus younger than the southwestern cluster. Summarized, an age progression from west to east can be inferred with ages of the diapirs ranging from Oligocene/Miocene (>23–10 Ma; reflections R3-R5) to late Miocene <10 Ma (reflections <R3), respectively.

Comparing ages of the extrapolated hotspot path of the SIH derived from absolute plate motion model WK08-D (Wessel & Kroenke 2008) with our age estimations for the formation of the diapirs, a good agreement of the southwestern cluster (23 Ma; blue volcanoes in Fig. 4) is observed. The igneous diapirs of the eastern cluster (brown volcanoes in Fig. 4) on average are about 5 Ma younger than the predicted ~15 Ma of model WK08-D. This age discrepancy can partly be explained by a coarse age resolution and the occurrence of unconformities, which hinder a linear interpolation between the dated seismic reflections R2–R3. Additionally, the absolute plate motion model WK08-D has uncertainties due to dating and the geometry is generally better modelled than age progression along a hotspot track (Wessel *et al.* 2006).

5.1.2 *Spatial distribution of diapirs*

A total number of 19 diapirs have been identified exclusively in the southern part of the High Plateau (Fig. 4, Table 2), whereas in the central part and along the southern, northeastern and western margins no diapirs could be identified. The diapirs solely occur in a narrow (~100 km), northwest to southeast striking corridor (Fig. 4), which suggests a spatially localized source. Its dimension is comparable to the growth and evolution of hotspots, like the recent SIH region, which has an areal extent of 100 km (Binard *et al.* 1991). Additionally, the diapirs are distributed parallel to the Neogene Pacific Plate motion (Fig. 4; Seton *et al.* 2012), which suggests that they display features of hotspot volcanism.

The distribution of diapirs deviates from a hypothetic hotspot path of the SIH path obtained from the absolute plate motion model WK08-D (Wessel & Kroenke 2008). This deviation can be explained by model uncertainties, because no data prior to 4.5 Ma (Duncan & McDougall 1976) have been included into the reconstruction model of the SIH path (Wessel *et al.* 2006). A comparison to well constrained hotspot tracks like the Hawaiian and Louisville hotspot tracks show predicted seamount corridors of 150 km, using model WK08-D (Wessel & Kroenke 2008).

In contrast, volcanism that is not driven by a point source cannot explain the distribution of diapirs for the following reason: The diapirs are not preferentially distributed within the entire southwestern and western High Plateau, which is an area that was strongly tectonically faulted by break-up processes of the Hikurangi Plateau (Davy *et al.* 2008) and southwestern extension due to the Palaeocene Plate

Table 2. Age and location of all diapirs identified in the entire Kiwi12 and So224 datasets across the High Plateau, subprovince of the Manihiki Plateau.

No.	Profile AWI-	CDPs		Dimens. (km)	Lat.	Lon.	Age (Ma)	Bounding reflections		Comments
1	20120013	3400	3470	1.8	−13.0047	−161.1277	10	R3	R4	Intrusion may be younger than R3 as reflection is still little bit disturbed.
2	20120016	4250	4450	5	−13.1200	−161.2477	<23	<R4	R4	
3	20120016	6250	6450	5	−13.3696	−161.5070	10	R3	R3	Extrusion, exhibiting double vents
4	20120016	6750	6850	2.5	−13.4243	−161.5643	10–23	<R4	R4	Small intrusion
5	20120017	2750	2900	3.8	−13.5210	−162.2713	∼23		R4?	Intrusion, disturbances visible until reflection R1
6	20120017	3300	3500	5.0	−13.5210	−162.4040	<23		<R4	Extrusion, no onlap structure visible
7	20120023	1134	1287	2.5	−12.4310	−163.2460	23–45		<R5	Small intrusion centre
8	20120023	1519	1633	2.9	−12.3491	−163.2470	<23	>R2	<R4	Big extrusion centre, elevation up to 250 m above seafloor, erosional unconformities within R3–R4
9	20120023	1953	2002	1.3	−12.2590	−163.2470	<45	>R2	<R5	Intrusion centre, erosional unconformities within R3–R4
10	20120028	1100	1200	2.5	−12.4340	−163.2970	10–45	>R3	<R5	Tectonic deformation of entire sediment column; dyke structure
11	20120201	4916	4996	4	−12.4720	−162.1070		R3	R3	Hydrothermal vent
12	20120201	7590	7669	4	−12.7320	−163.2530	10–45	R3	R5	
13	20120201	6982	7047	3.3	−12.6710	−162.9900	23–45	R4	R5	Formation age between R4–R5
14	Kiwi1204	5480	5540	2.7	−12.6311	−163.2216	<45	?	R5	Upward bent and disturbed reflections R7–R5; strong tectonic deformation in Units 3 and 4
15	Kiwi1206	5850	5900	2.2	−13.0575	−161.9458	<23	<R3	R4	Intrusion got stuck at R3–R4; disturbed upper reflection sequence
16	Kiwi1206	5680	5730	2.2	−13.1134	−161.9750	> 5.3 <23		R3	Intrusion got stuck at R3–R4
17	Kiwi1207	11 590	11 625	1.6	−13.0717	−161.3973	10–23	R3	R4	Upward bent reflections R7–R4; onlap structure at R3
18	Kiwi1207	12 340	12 380	1.8	−13.1952	−161.6828	?			Amplitude destruction of entire sedimentary column, side reflection?
19	Kiwi1207	12 700	12 735	1.6	−13.3516	−161.7498	34	>R4	<R5	
20	Kiwi1211	3905	3945	1.8	−9.5178	−161.0865			<R6	

reorganization (Pietsch & Uenzelmann-Neben 2016). The resulting disturbed volcanic basement (Units 3 and 4) promotes potential pathways for ascending magma, preferentially along ancient sills and dykes (Le Corvec *et al.* 2013). Therefore, one would expect an increased occurrence of diapirs at the entire southwestern High Plateau, which is not observed.

Summarizing, we have identified igneous diapirs within the southern High Plateau, which were formed during the Neogene and appear unrelated to the initial Cretaceous volcanic formation period. Their apparent age progression and spatial distribution suggest a hotspot volcanic origin, which might originate from plume activity or shear-stress derived volcanism. An extrapolation of the SIH track (Fig. 4) using model WK08-D (Wessel & Kroenke 2008) shows a crossing of the HP during the Miocene, but no independent geological data exist to confirm this model. Although, we cannot rule out a shear-stress derived source, we suggest that the igneous diapirs may represent a western extension of the SIH due to good conformities of observed diapirs and extrapolated hotspot path.

5.2 Implications and comparison to other LIPs

Hotspot volcanism has so far hardly been studied within LIP crust. The identified diapirs within the MP provide a unique setting to study the influence of localized volcanism within a LIP that is not related to volcanism of the initial formation period.

In the previous sections it has been shown that the igneous diapirs are possibly expressions of hotspot volcanism. Similar structures are revealed across the Kerguelen Plateau, a Cretaceous LIP (∼130 Ma) in the Indian Ocean (Coffin *et al.* 2002) that crossed the Kerguelen-Heard plume (Oligocene to recent; Mahoney *et al.* 1983; Weis & Frey 1996). Samples of dredged submarine volcanoes have revealed an apparent age trend from north to south between 34 Ma in the Northern Kerguelen Plateau up to 18–21 Ma that may correspond to the Tertiary hotspot track of the Kerguelen Plateau (Weis *et al.* 2002). Diapirs (there referred to as piercement structures) can be observed in seismic reflection data north of Heard Islands (Ramsay *et al.* 1986), the assumed present day hotspot location (Weis & Frey 1996) and are absent in the southern profiles. Appearance and spatial extent of these subvolcanic intrusives (Ramsay *et al.* 1986) are comparable to the newly detected diapirs of the MP. Assuming a hotspot origin for the Kerguelen piercement structures, we conclude that 'late stage' hotspot volcanism within a LIP is generally displayed by narrow, localized diapirs of small spatial extent, which is different to hotspot volcanism seen within oceanic lithosphere, where continuous seamount chains are formed, seen for example, for the Society Islands (e.g. Payne *et al.* 2013).

A possible explanation is provided by the anomalous crustal thickness of up to 20 km of the HP, which is two to three times thicker than normal oceanic lithosphere. Petrological studies (Nixon 1980; Ishikawa 2011) of the Ontong Java Plateau (OJP), reveal an occurrence of kimberlite-like magmas. Although kimberlites are in general considered to be formed by an interaction of a plume with continental crust, the studies on the OJP suggest that an interaction of the anomalously thick LIP crust with ascending magma of a plume results in similar chemical signatures (Nixon 1980; Ishikawa 2011). A comparison to hotspot volcanism seen within tectonically faulted continental crust, for example at the Walvis Ridge (Fromm *et al.* 2015), shows that hotspot volcanism is restricted to a distinct, small area that is located above the assumed hotspot path. We conclude that LIP crust, although different in composition and

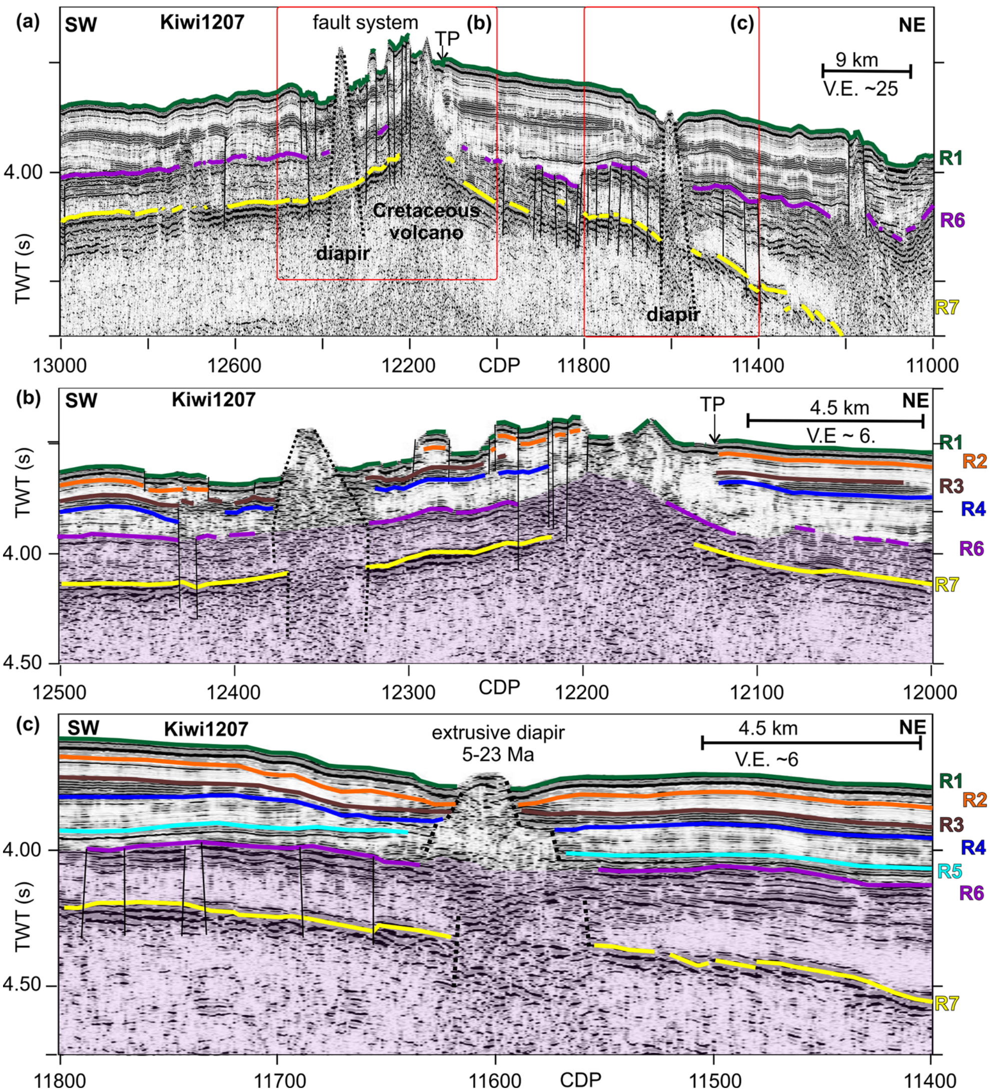

Figure 6. Seismic reflection profile Kiwi07 in the southeastern part of the High Plateau (a) and enlargements (b and c) showing two well-defined diapirs and a tectonic fault system on top of a Cretaceous volcanic centre.

thickness, acts more like continental crust when interacting with hotspot magmatism.

6 CONCLUSIONS

We have investigated late Eocene to Miocene magmatism in the High Plateau a subprovince of the MP, a LIP in the central Pacific. A dense cluster of high resolution seismic reflection data (So224) and single channel seismic reflection data (Kiwi12) were used with a geochronology derived from a correlation to drill hole at Site 317 from DSDP Leg 33 (Pietsch & Uenzelmann-Neben 2015).

A total number of 19 igneous diapirs has be identified, exclusively in the southern High Plateau, which are characterized by (i) an occurrence of narrow diapirs with small lateral extent (<5 km), (ii) classification into extrusion and intrusion centres based on occurrence of onlap structures of sediments that accumulated after the diapirs were formed, (iii) an exclusive occurrence within a narrow WNW–SSE striking corridor, parallel to the Neogene Pacific Plate motion (Seton *et al.* 2012) and (iv) a grouping into a southwestern and southeastern cluster with different average ages of 23–10 Ma and 10→ 5.3 Ma, implying that volcanism becomes younger towards the east. We conclude that the igneous diapirs are hotspot-related and were fed by a distinct, spatially localized source. The distribution of the diapirs overlaps with an assumed extrapolation of the SIH track between ∼22 and ∼15 Ma. We suggest that we thus have identified a previously unknown expression of the SIH that extends the known reconstructed path from 4.5 Ma on Maupiti to 23 Ma on the MP. A comparison of igneous diapirs to hotspot volcanism within oceanic lithosphere further suggests that LIP crust interact with ascending hotspot magma differently to oceanic crust and more similar to continental crust.

ACKNOWLEDGEMENTS

We want to express our gratitude to Captain Lutz Mallon and his officers and crew of RV *Sonne* for their professional and enthusiastic engagement and service during the scientific program of this leg. We further thank the editor and two anonymous reviewers for their helpful comments. We are grateful to Joann Stock and Bruce Luyendyk for providing access to the seismic data collected during RV *Revelle* cruise Kiwi Leg 12 via http://www.ig.utexas.edu.sdc. Data of cruise leg So224 will be published at Pangea database http://pangaea.de/search?ie=UTF-8&env=All&count=10&q=So224 in about 2 years due to legal requirements. This cruise leg So224 and the project Manihiki II are primarily funded by the German Federal Ministry of Education and Research (BMBF) under Project Number 03G0224A. Additional funding has been provided by the Alfred-Wegener-Institute.

REFERENCES

Adam, C., Yoshida, M., Isse, T., Suetsugu, D., Fukao, Y. & Barruol, G., 2010. South Pacific hotspot swells dynamically supported by mantle flows, *Geophys. Res. Lett.,* **37,** L08302, doi:10.1029/2010GL042534.

Ai, H.-A., Stock, J., Clayton, R. & Luyendyk, B., 2008. Vertical tectonics of the High Plateau region, Manihiki Plateau, Western Pacific, from seismic stratigraphy, *Mar. geophys. Res.,* **29**(1), 13–26.

Anderson, D.L., 2000. The thermal state of the upper mantle; no role for mantle plumes, *Geophys. Res. Lett.,* **27**(22), 3623–3626.

Ballmer, M.D., Conrad, C.P., Smith, E.I. & Harmon, N., 2013. Non-hotspot volcano chains produced by migration of shear-driven upwelling toward the East Pacific Rise, *Geology,* **41**(4), 479–482.

Barruol, G., Suetsugu, D., Shiobara, H., Sugioka, H., Tanaka, S., Bokelmann, G.H.R., Fontaine, F.R. & Reymond, D., 2009. Mapping upper mantle flow beneath French Polynesia from broadband ocean bottom seismic observations, *Geophys. Res. Lett.,* **36,** doi:10.1029/2009GL038139.

Billen, M.I. & Stock, J., 2000. Morphology and origin of the Osbourn Trough, *J. geophys. Res.,* **105**(B6), 13 481–13 489.

Binard, N., Hékinian, R., Cheminée, J.L., Searle, R.C. & Stoffers, P., 1991. Morphological and structural studies of the Society and Austral hotspot regions in the South Pacific, *Tectonophysics,* **186**(3–4), 293–312.

Binard, N., Maury, R.C., Guille, G., Talandier, J., Gillot, P.Y. & Cotten, J., 1993. Mehetia Island, South Pacific: geology and petrology of the emerged part of the Society hot spot, *J. Volc. Geotherm. Res.,* **55**(3–4), 239–260.

Chandler, M.T., Wessel, P., Taylor, B., Seton, M., Kim, S.-S. & Hyeong, K., 2012. Reconstructing Ontong Java Nui: implications for Pacific absolute plate motion, hotspot drift and true polar wander, *Earth planet. Sci. Lett.,* **331–332,** 140–151.

Clouard, V. & Bonneville, A., 2001. How many Pacific hotspots are fed by deep-mantle plumes?, *Geology,* **29**(8), 695–698.

Clouard, V. & Gerbault, M., 2008. Break-up spots: could the Pacific open as a consequence of plate kinematics?, *Earth planet. Sci. Lett.,* **265**(1–2), 195–208.

Coffin, M.F., Pringle, M.S., Duncan, R.A., Gladczenko, T.P., Storey, M., Muller, R.D. & Gahagan, L.A., 2002. Kerguelen hotspot magma output since 130 Ma, *J. Petrol.,* **43**(7), 1121–1139.

Davy, B., 2014. Rotation and offset of the Gondwana convergent margin in the New Zealand region following Cretaceous jamming of Hikurangi Plateau large igneous province subduction, *Tectonics,* **33**(8), 1577–1595.

Davy, B., Hoernle, K. & Werner, R., 2008. Hikurangi Plateau: crustal structure, rifted formation, and Gondwana subduction history, *Geochem. Geophys. Geosyst.,* **9**(7), doi:10.1029/2007GC001855.

Duncan, R.A. & McDougall, I., 1976. Linear volcanism in French Polynesia, *J. Volc. Geotherm. Res.,* **1**(3), 197–227.

Foulger, G.R. & Natland, J.H., 2003. Is "hotspot" volcanism a consequence of plate tectonics?, *Science,* **300**(5621), 921–922.

Fromm, T., Planert, L., Jokat, W., Ryberg, T., Behrmann, J.H., Weber, M.H. & Haberland, C., 2015. South Atlantic opening: a plume-induced breakup?, *Geology,* **43**(10), 931–934.

Gaboret, C., Forte, A.M. & Montagner, J.P., 2003. The unique dynamics of the Pacific Hemisphere mantle and its signature on seismic anisotropy, *Earth planet. Sci. Lett.,* **208**(3–4), 219–233.

Gripp, A.E. & Gordon, R.G., 1990. Current plate velocities relative to the hotspots incorporating the Nuvel-1 Global Plate Motion Model, *Geophys. Res. Lett.,* **17**(8), 1109–1112.

Gripp, A.E. & Gordon, R.G., 2002. Young tracks of hotspots and current plate velocities. *Geophys. J. Int.,* **150**(2), 321–361.

Hieronymus, C.F. & Bercovici, D., 2000. Non-hotspot formation of volcanic chains: control of tectonic and flexural stresses on magma transport, *Earth planet. Sci. Lett.,* **181**(4), 539–554.

Hochmuth, K., Gohl, K. & Uenzelmann-Neben, G., 2015. Playing jigsaw with Large Igneous Provinces—a plate tectonic reconstruction of Ontong Java Nui, West Pacific, *Geochem. Geophys. Geosyst.,* **16**(11), 3789–3807.

Hoernle, K., Hauff, F., van den Bogaard, P., Werner, R., Mortimer, N., Geldmacher, J., Garbe-Schonberg, D. & Davy, B., 2010. Age and geochemistry of volcanic rocks from the Hikurangi and Manihiki oceanic Plateaus, *Geochim. Cosmochim. Acta,* **74**(24), 7196–7219.

Hussong, D.M., Wipperman, L.K. & Kroenke, L.W., 1979. Crustal structure of the Ontong Java and Manihiki Oceanic Plateaus, *J. geophys. Res.,* **84**(Nb11), 6003–6010.

Ingle, S., Mahoney, J., Sato, H., Coffin, M., Kimura, J., Hirano, N. & Nakanishi, M., 2007. Depleted mantle wedge and sediment fingerprint in unusual basalts from the Manihiki Plateau, central Pacific Ocean, *Geology,* **35**(7), 595–598.

Ishikawa, A., 2011. Spectacular mantle xenoliths derived from "Oceanic Kimberlite", Malaita, Solomon Islands: a unique window into the Earth's deep interior, *J. Geograph. (Chigaku Zasshi),* **120**(6), 1026–1034.

Jackson, C.A.-L., 2012. Seismic reflection imaging and controls on the preservation of ancient sill-fed magmatic vents, *J. Geol. Soc.,* **169**(5), 503–506.

Kopp, H., Kopp, C., Morgan, J.P., Flueh, E.R., Weinrebe, W. & Morgan, W.J., 2003. Fossil hot spot-ridge interaction in the Musicians Seamount Province: geophysical investigations of hot spot volcanism at volcanic elongated ridges, *J. geophys. Res.,* **108**(B3), doi:10.1029/2002JB002015.

Koppers, A.A.P. & Staudigel, H., 2005. Asynchronous bends in Pacific seamount trails: a case for extensional volcanism?, *Science,* **307**(5711), 904–907.

Koppers, A.A.P., Staudigel, H., Pringle, M.S. & Wijbrans, J.R., 2003. Short-lived and discontinuous intraplate volcanism in the South Pacific: hot spots or extensional volcanism?, *Geochem. Geophys. Geosyst.,* **4**(10), doi:10.1029/2003GC000533.

Koppers, A.A.P., Staudigel, H., Phipps Morgan, J. & Duncan, R.A., 2007. Nonlinear ^{40}Ar/^{39}Ar age systematics along the Gilbert Ridge and Tokelau Seamount Trail and the timing of the Hawaii-Emperor Bend, *Geochem. Geophys. Geosyst.,* **8**(6), doi:10.1029/2006GC001489.

Lancelot, Y. & Embley, R., 1977. Piercement structures in deep oceans. *AAPG Bull.,* **61**(11), 1991–2000.

Lanphere, M.A. & Dalrymple, G.B., 1976. K-AR Ages of basalts from DSDP Leg 33: Sites 315 (Line Island) and 317 (Manihiki Plateau), in *Initial Reports of the Deep Sea Drilling Project,* Vol. 33, pp. 649–653, ed. Kaneps, A.G., US Governmental Printing Office.

Larson, R.L. & Erba, E., 1999. Onset of the mid-Cretaceous greenhouse in the Barremian-Aptian: igneous events and the biological, sedimentary, and geochemical responses, *Paleoceanography,* **14**(6), 663–678.

Larson, R.L., Pockalny, R.A., Viso, R.F., Erba, E., Abrams, L.J., Luyendyk, B.P., Stock, J.M. & Clayton, R.W., 2002. Mid-Cretaceous tectonic evolution of the Tongareva triple junction in the southwestern Pacific Basin, *Geology,* **30**(1), 67–70.

Le Corvec, N., Menand, T. & Lindsay, J., 2013. Interaction of ascending magma with pre-existing crustal fractures in monogenetic basaltic volcanism: an experimental approach, *J. geophys. Res.: Solid Earth,* **118**(3), 968–984.

Mahoney, J.J., Macdougall, J.D., Lugmair, G.W. & Gopalan, K., 1983. Kerguelen hotspot source for Rajmahal Traps and Ninetyeast Ridge?, *Nature,* **303**(5916), 385–389.

Mahoney, J.J., Storey, M., Duncan, R.A., Spencer, K.J. & Pringle, M., 1993. Geochemistry and age of the Ontong Java Plateau, in *The Mesozoic Pacific: Geology, Tectonics, and Volcanism*, pp. 233–261, eds Pringle, M.S., Sager, W.W., Sliter, W.V. & Stein, S., American Geophysical Union.

Morgan, W.J., 1972. Deep mantle convection plumes and plate motions, *Am. Assoc. Pet. Geol. Bull.,* **56**(2), 203–213.

Nakanishi, M., Nakamura, Y., Coffin, M.F., Hoernle, K. & Werner, R., 2015. Topographic expression of the Danger Islands Troughs and implications for the tectonic evolution of the Manihiki Plateau, western equatorial Pacific Ocean, *Geol. Soc. Am. Spec. Papers,* **511,** 195–220.

Neall, V.E. & Trewick, S.A., 2008. The age and origin of the Pacific islands: a geological overview, *Phil. Trans. R. Soc. B-Biol. Sci.,* **363**(1508), 3293–3308.

Nixon, P.H., 1980. Kimberlites in the south-west Pacific, *Nature,* **287**(5784), 718–720.

O'Connor, J.M. *et al.*, 2015. Deformation-related volcanism in the Pacific Ocean linked to the Hawaiian-Emperor bend, *Nat. Geosci.,* **8**(5), 393–397.

Payne, J.A., Jackson, M.G. & Hall, P.S., 2013. Parallel volcano trends and geochemical asymmetry of the Society Islands hotspot track, *Geology,* **41**(1), 19–22.

Pietsch, R. & Uenzelmann-Neben, G., 2015. The Manihiki Plateau—a multi-stage volcanic emplacement history, *Geochem. Geophys. Geosyst.,* **16**(8), 2480–2498.

Pietsch, R. & Uenzelmann-Neben G., 2016. Paleocene Pacific Plate reorganization mirrored in formation of the Suvarov Trough, Manihiki Plateau, *J. geophys. Res.: Solid Earth Planets,* in press.

Ramsay, D.C., Colwell, J.B., Coffin, M.F., Davies, H.L., Hill, P.J., Pigram, C.J. & Stagg, H.M.J., 1986. New findings from the Kerguelen Plateau, *Geology,* **14**(7), 589–593.

Seton, M. *et al.*, 2012. Global continental and ocean basin reconstructions since 200 Ma. *Earth Sci. Rev.,* **113**(3–4), 212–270.

Sharp, W.D. & Clague, D.A., 2006. 50-Ma initiation of Hawaiian-Emperor bend records major change in Pacific plate motion, *Science,* **313**(5791), 1281–1284.

Shipboard Scientific Party, 1976. Site 317, in *Initial reports of the Deep Sea Drilling Project,* Vol. 33, pp. 161–300, ed. Kaneps, A.G., US Governmental Printing Office.

Suetsugu, D. & Hanyu, T., 2013. Origin of hotspots in the South Pacific: Recent advances in seismological and geochemical models, *Geochem. J.,* **47**(2), 259–284.

Suetsugu, D. *et al.*, 2009. South Pacific mantle plumes imaged by seismic observation on islands and seafloor, *Geochem. Geophys. Geosyst.,* **10,** doi:10.1029/2009GC002533.

Tanaka, S., Suetsugu, D., Shiobara, H., Sugioka, H., Kanazawa, T., Fukao, Y., Barruol, G. & Reymond, D., 2009a. On the vertical extent of the large low shear velocity province beneath the South Pacific Superswell, *Geophys. Res. Lett.,* **36,** doi:10.1029/2009GL037568.

Tanaka, S. *et al.*, 2009b. P-wave tomography of the mantle beneath the South Pacific Superswell revealed by joint ocean floor and islands broadband seismic experiments, *Phys. Earth planet. Inter.,* **172**(3–4), 268–277.

Taylor, B., 2006. The single largest oceanic plateau: Ontong Java-Manihiki-Hikurangi, *Earth planet. Sci. Lett.,* **241**(3–4), 372–380.

Timm, C., Hoernle, K., Werner, R., Hauff, F., v. den Bogaard, P., Michael, P., Coffin, M.F. & Koppers, A., 2011. Age and geochemistry of the oceanic Manihiki Plateau, SW Pacific: new evidence for a plume origin, *Earth planet. Sci. Lett.,* **304**(1–2), 135–146.

Uenzelmann-Neben, G., 2012. The Expedition of the Research Vessel "Sonne" to the Manihiki Plateau in 2012 (SO 224), in *Reports on Polar and Marine Research*, ed. Uenzelmann-Neben, G., Alfred-Wegener-Institut für Polar- und Meeresforschung in der Helmholtz Gemeinschaft.

Uto, K., Yamamoto, Y., Sudo, M., Uchiumi, S., Ishizuka, O., Kogiso, T. & Tsunakawa, H., 2007. New K-Ar ages of the Society Islands, French Polynesia, and implications for the Society hotspot feature, *Earth, Planets Space,* **59**(7), 879–885.

Weatherall, P. *et al.*, 2015. A new digital bathymetric model of the world's oceans, *Earth Space Sci.,* **2**(8), 331–345.

Weis, D. & Frey, F.A., 1996. Role of the Kerguelen Plume in generating the eastern Indian Ocean seafloor, *J. geophys. Res.: Solid Earth,* **101**(B6), 13 831–13 849.

Weis, D. *et al.*, 2002. Trace of the Kerguelen mantle plume: evidence from seamounts between the Kerguelen Archipelago and Heard Island, Indian Ocean, *Geochem. Geophys. Geosyst.,* **3**(6), 1–27.

Wessel, P. & Kroenke, L.W., 2007. Reconciling late Neogene Pacific absolute and relative plate motion changes, *Geochem. Geophys. Geosyst.,* **8,** doi:10.1029/2007GC001636.

Wessel, P. & Kroenke, L.W., 2008. Pacific absolute plate motion since 145 Ma: an assessment of the fixed hot spot hypothesis, *J. geophys. Res.,* **113**(B6), doi:10.1029/2007JB005499.

Wessel, P., Harada, Y. & Kroenke, L.W., 2006. Toward a self-consistent, high-resolution absolute plate motion model for the Pacific, *Geochem. Geophys. Geosyst.,* **7,** doi:10.1029/2005GC001000.

Worthington, T.J., Hekinian, R., Stoffers, P., Kuhn, T. & Hauff, F., 2006. Osbourn Trough: structure, geochemistry and implications of a mid-Cretaceous paleospreading ridge in the South Pacific, *Earth planet. Sci. Lett.,* **245**(3–4), 685–701.